

Fluctuating Spinodal-like Structure in the Glacial Phase of D-Mannitol

Published as part of *The Journal of Physical Chemistry B* special issue “Mark Ediger Festschrift”.

Jianing Wang, Lijian Song,* Xiao Chen, Xiao Jin, Meng Gao, Juntao Huo, and Jun-Qiang Wang*



Cite This: *J. Phys. Chem. B* 2025, 129, 540–545



Read Online

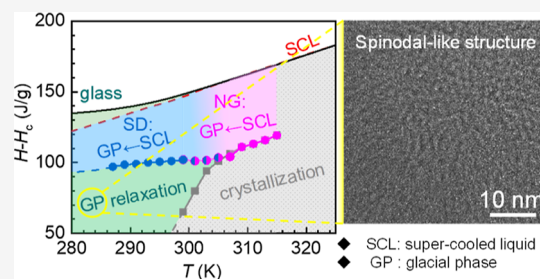
ACCESS |

Metrics & More

Article Recommendations

Supporting Information

ABSTRACT: The glacial phase can be formed from supercooled liquid (SCL) in certain systems, which is called liquid–liquid transition (LLT). Revealing the nature of the glacial phase especially in a single-component system is crucial for understanding the LLT process. Here, by using flash differential scanning calorimetry and cold-field transmission electron microscopy, the structure of the D-mannitol glacial phase and the phase transition kinetics between the glacial phase and SCL were studied. We found that the glacial phase is a fluctuating spinodal-like structure. And the glacial phase displays a first-order melting characteristic when it transforms into the SCL. Furthermore, the LLT diagram in the enthalpy–temperature coordinate system is constructed based on the nucleation–growth and spinodal-decomposition transitions. Our findings provide new insight into the LLT process of the glass forming liquids.



INTRODUCTION

When a melt is cooled below its solidification point, it will enter a super-cooled liquid (SCL) equilibrium state.^{1,2} If held isothermally, SCL usually crystallizes. However, in certain systems, such as water,^{3,4} triphenyl phosphate^{5,6} (TPP), D-mannitol,^{7,8} and some metallic glass formers,^{9–13} the SCL can undergo a transformation into another amorphous phase, which is known as “liquid–liquid transition” (LLT). LLT involves the transition between two disordered states without any change in long-range order.¹¹ And notably, the LLT here actually describes the transformation of a liquid into a glassy state of another liquid, regardless of whether the final is in a glass or liquid state.^{6,14} This definition was adopted for simplification and has since gained widespread acceptance.^{10,15} Revealing the nature of the LLT is crucial to understanding the phase transition of glassy systems.

To describe the LLT in glasses, Kivelson and his colleagues first proposed to use the “glacial phase” to analyze the end state of LLT in TPP molecular liquid because of the “amorphous” character with a wide X-ray scattering peak.⁵ Recently, Tanaka et al. demonstrated the reversibility and first-order nature of the LLT in the TPP by using flash differential scanning calorimetry (DSC),¹⁴ ruling out the possibility that the glacial phase contains undetectable nanocrystals. And in metallic glasses, the packing of the medium-range order structure of LLT revealed by transmission electron microscopy (TEM) suggests that the glacial phase is characterized by the implicit order structure or nanocrystal-like structure.^{9,11} Nevertheless, the structural characterization of the glacial phase, especially in single-component molecular liquids, is still unclear.

The transition between the glacial phase and the SCL has also been a long-standing topic of interest over the past decade. Recent simulation results have shown that the glacial phase displays a first-order melting transition to the SCL at a coexistence temperature.¹⁶ And the glacial phase needs to transform into the liquid before crystallizing.¹⁷ This insight suggests that the glacial phase of SCL has melting characteristics. On the other hand, Perepezko et al. discovered a broad exothermic peak during the LLT process, which exhibits similar kinetics to crystallization.^{8,15} Given a strong link between the glacial phase and crystallization, understanding the kinetics of the glacial phase is essential for drawing the glass–liquid transition.

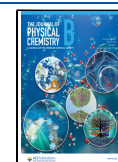
In this work, the LLT behaviors of D-mannitol are studied. The formation thermodynamics of the glacial phase are studied using a high-precision flash differential scanning calorimeter. The nanostructure of the glacial phase is studied using high-resolution transmission microscopy (TEM), which shows a fluctuating spinodal-like structure. And its transition to the SCL displays first-order melting character.

Received: September 22, 2024

Revised: November 27, 2024

Accepted: December 13, 2024

Published: December 23, 2024



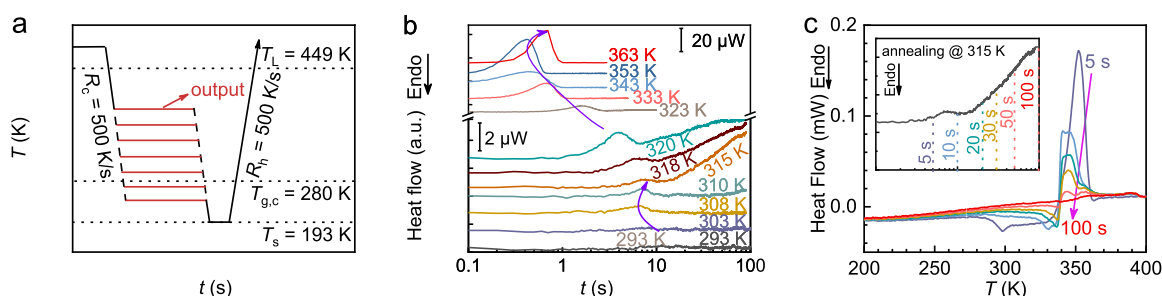


Figure 1. (a) The thermal protocol of flash differential scanning calorimetry (DSC) for isothermal annealing. (b) The typical isothermal heat flow curves at different annealing temperatures T_a ; the purple arrows are guide lines. (c) Reheating heat flow curves after annealing at 315 K for different annealing times t_a . The inset shows the isothermal heat flow curve annealed at 315 K, where the colors of different t_a correspond to the colors of reheated heat flow curves.

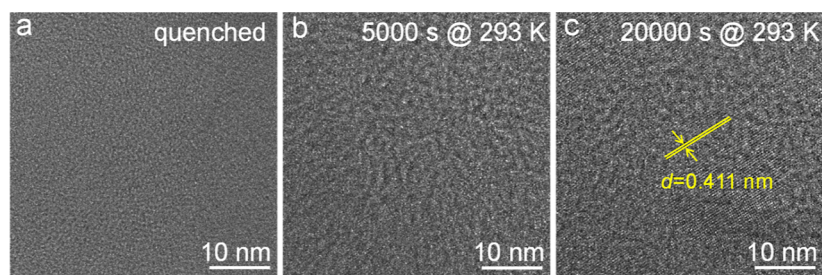


Figure 2. High-resolution transmission electron microscopy images of the D-mannitol glass with different annealing conditions (a) quenched; (b) annealed 5000 s at 293 K; (c) annealed 20,000 s at 293 K.

EXPERIMENTAL SECTION

D-Mannitol (99.9999% purity) was purchased from Sigma-Aldrich. Thermal analyses were conducted with a Mettler Toledo Flash DSC 1 with a mechanical pump refrigeration system and nitrogen purge. The D-mannitol particle with an appropriate size was selected and loaded on the flash DSC chip under an optical microscope. The heat capacity C_p was calculated by the formula: $C_p = \frac{\dot{Q}}{Rm}$, where \dot{Q} is the heat flow that can be detected directly by flash DSC. R is the scanning rate. And m is the mass of the sample, which was estimated by measuring the melting enthalpy and normalized by the specific melting enthalpy of 293 J/g.⁷

The structural characterization was performed using a Tecnai F20 TEM with a field emission of 200 kV. The D-mannitol sample was sealed in an Al crucible, fully re-melted at 473 K, and then rapidly quenched in liquid nitrogen. This cooling rate was sufficient to obtain a completely amorphous D-mannitol sample.⁷ And the glacial phase glass was produced by annealing quenched glass at 293 K. The quenched and glacial phase glass were dispersed in ether, respectively, and the ultrasonic treatment was performed for 10 min to ensure uniform dispersion. A pipet was then used to deposit a small amount of the sample solution onto a copper grid with a carbon film. Finally, the copper grid with the sample was loaded onto the TEM sample holder for observation and analysis.

RESULTS AND DISCUSSION

Figure 1a shows the thermal protocol of flash DSC for isothermal annealing. Generally, the SCL of D-mannitol undergoes a transition to the glacial phase when annealing below 320 K, while crystallization occurs above this temperature.¹⁵ To reveal the kinetics of the glacial phase formation and crystallization, the D-mannitol melt was cooled from 473

K, which was above the liquid temperature $T_L = 449$ K, to different annealing temperatures (T_a) at a cooling rate $R_c = 500$ K/s. The T_a ranged from 273 to 363 K, which encompassed both the crystallization and glacial phase formation temperatures. Finally, the samples were cooled to 193 K and then reheated to 473 K at a heating rate $R_h = 500$ K/s.

The isothermal heat flow curves at T_a are shown in Figure 1b. It can be found that the SCL crystallized at $T_a \geq 323$ K, exhibiting a classic C-shaped transformation. However, when T_a was below 323 K, the isothermal heat flow curves showed a slow exothermic reaction after an exothermic peak. With the T_a continuing to decrease, a new C-shaped curve appeared, representing the formation of the glacial phase.¹⁵ If T_a was below 293 K, no obvious exothermic peaks were detected, though the glacial phase still formed. This confirms the existence of two distinct mechanisms for the glacial phase formation.^{6,15} Additionally, to verify what happened in the slow exothermic reaction at 315 K, the isothermal annealing process was interrupted by annealed different $t_a = 5, 10, 20, 30, 50, 100$ s, and then the sample was cooled to 193 K and reheated. The reheated heat flow curves are shown in Figure 1c. As the isothermal heat flow curve shifted upward, the sample crystallized, evidenced by the gradual decrease of the crystallization peak area. Additionally, the reheating heat flow curves with shorter t_a exhibit an extra endothermic peak occurring around 320–340 K before crystallization, which coincides with the temperature range for the transition of the glacial phase to SCL. This indicates that a partial glacial phase also formed at this stage. Thus, it can be conjectured that the first peak at 315 K primarily corresponds to the formation of the glacial phase, and crystallization also occurs. The appearance of the glacial phase causes the crystallization heat flow curve to deviate from the typical peak shape, instead showing a gradual upward shift.

The heat flow curves of D-mannitol after being annealed at $T_a = 273, 283, 293$, and 303 K are shown in Figure S1. When being annealed well below T_g , e.g., 273 K, the glass exhibits a typical aging process. The endothermic overshoot at T_g increases and shifts to a higher temperature until it gets to an equilibrium state. When being annealed at higher temperatures, e.g., 283 – 303 K, the glass will transform into a glacial phase after reaching the equilibrium state. The evolution of the microstructure after being annealed at 293 K was studied using high-resolution TEM (HRTEM), as shown in Figure 2. The as-quenched glass exhibits a typical disordered molecular packing structure. For the sample annealed at 293 K for 5000 s to form the glacial phase, as shown in Figure 2b, the HRTEM image still displays a disordered structure without any observed lattice fringes. Nevertheless, the sample exhibits a more heterogeneous structure compared to the quenched glass, showing a fluctuating spinodal-like structure. This provides direct experimental evidence for the existence of a spinodal-type LLT proposed by previous studies.^{6,14,15} When the t_a reached 20000 s, HRTEM reveals distinct lattice fringes, with a calculated interplanar spacing of $d = 0.411$ nm. Therefore, it can be inferred that this spinodal-like structure represents an intermediate state between the disordered glass and crystal. Previous studies have suggested that SCL will be intrinsically heterogeneous before crystallization, characterized as a spinodal structure by density and orientational fluctuations.^{18–20} Our findings provide strong experimental evidence supporting this viewpoint.

Since the glacial phase is determined with a fluctuating spinodal-like structure, it is necessary to analyze its transition process to the SCL. One of the longstanding controversies in this transition is the recovery experiment. For the ordinary annealed glass, as shown in Figure 3a, the gray dashed line represents the heat flow curve of the sample annealed at 273 K for $t_a = 100$ s, exhibiting an endothermic overshoot at the glass transition temperature. When the annealed glass was heated to the recovery temperature ($T_{re} = 300$ K) before the end of the overshoot, the reheating curve of the cooled sample exhibited a small overshoot with its peak shifting to a lower temperature. This phenomenon indicates that the energy state is restored after the reaction mixture has been heated to T_{re} . However, as shown in Figure 3b, when the glacial phase was heated to $T_{re} = 327$ K and then cooled, the reheating curve exhibited two peaks. The first peak is the glass transition of the ordinary glass obtained upon cooling from the SCL. The second peak corresponds to the transformation of the residual glacial phase to SCL. The peak of the residual glacial phase shifts toward a higher temperature after recovery, while the overshoot of the aged ordinary glass shifts to a lower temperature after recovery. Considering the partial melting process shown in Figure S2, the re-melting peak shifts to a higher temperature because crystal grains grow larger.^{21,22} Therefore, it is reasonable to conjecture that the endothermic peak of the transition from glacial phase to SCL is actually a melting behavior, where the spinodal-like structure evanishes. The above result is consistent with previous simulation results.^{16,17} Moreover, the crystallization behavior during cooling of the SCL obtained from the glacial phase and as-cooled glass are compared. As shown in Figure 3c,d, the samples were heated to the same temperature $T = 339$ K and then cooled at a rate of 50 K/s. The SCL derived from the glacial phase has a larger crystallization peak, indicating that it crystallized more easily. Furthermore, the as-

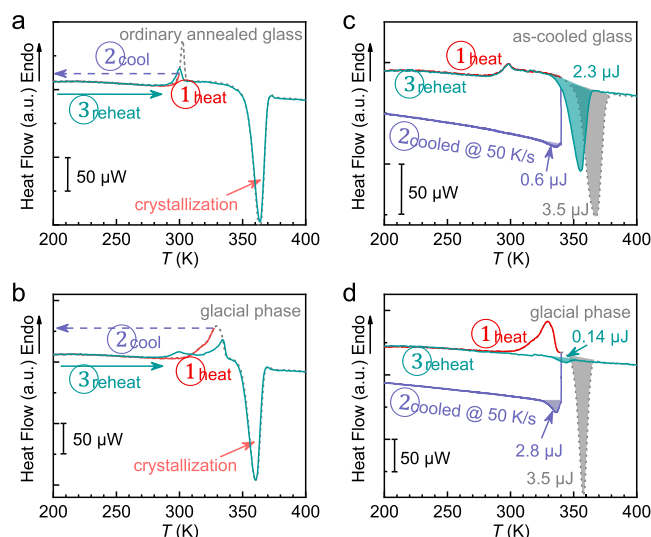


Figure 3. (a,b) The heat flow curves for (a) the ordinary annealed glass annealed at 273 K for $t_a = 100$ s and (b) the glacial phase annealed at 293 K for $t_a = 100$ s. The gray dashed lines represent the heating curves of the sample. ①: The red lines represent the heating process of the sample heated to the recovery temperature T_{re} . ②: The purple dotted arrows represent the samples cooled to 193 K at a cooling rate of 500 K/s. ③: The green lines represent the reheating curve of the recovery sample. (c,d) The crystallization behavior during cooling after (c) the as-cooled glass and (d) the glacial phase transition to the supercooled liquid (SCL). The gray dashed lines represent the heating curves of the sample. The red lines represent the heating process of the sample until it transitions to SCL. The purple lines represent the cooling curves of the SCL at a rate of 50 K/s. And the green lines represent the reheating curve of the sample after the cooling process.

cooled glass exhibited a crystallization peak on reheating, while a minor peak was displayed in the glacial phase.

Additionally, the crack healing experiment was performed to further reveal the difference between the glacial phase and the SCL. As shown in Figure 4a, when D-sorbitol was heated above its glass transition temperature (T_g), the cracks showed obvious healing contributed by its fluidity. Figure 4b shows the crack healing of D-mannitol at 288 K. It can be observed that small cracks were healed in a short time, while large cracks barely changed. However, there was almost no apparent crack healing of D-mannitol at 299 K shown in Figure 4c. Considering that the SCL of D-mannitol will transform into a glacial phase at this temperature range, it indicates that the glacial phase has greater viscosity and exhibits solid behavior, leading to the inability of cracks to heal. The healing of small cracks at 288 K is attributed to the mobility of SCL which has not completely transformed into a glacial phase. At a higher temperature of 299 K, SCL rapidly transforms into a glacial phase, resulting in insignificant crack healing.

Finally, the isothermal transformation of SCL was studied to analyze the kinetics of LLT at different temperatures, as shown in Figure 5a. The SCL crystallized directly at temperatures above 323 K, which shows a typical C-type temperature–time–transformation (TTT) curve. When the temperature decreased to below 313 K, the SCL transformed into a glacial phase first and then crystallized. The TTT curve for the formation of the glacial phase was also C-type with a nose at about 309 K. The glass transition happened at about $T_g = 297$ K. It is well known that the characteristic time for α relaxation is about $\tau_\alpha = 100$ s

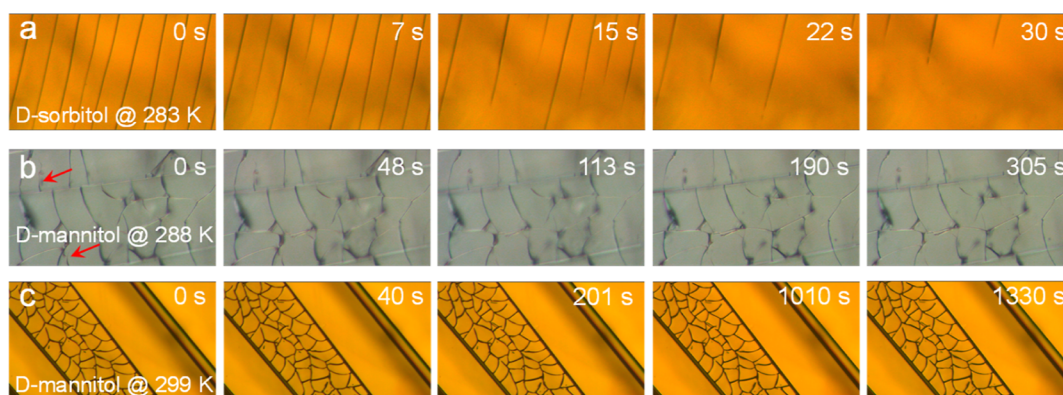


Figure 4. (a–c) The crack self-healing process of (a) D-sorbitol at 283 K, (b) D-mannitol at 288 K, and (c) D-mannitol at 299 K. The melt contained in two glasses with about 10 μm in thickness was quenched by liquid N_2 , picked up, and then moved to a copper cube under an optical microscope. The transfer process is less than 2 s. The temperature of the copper cube is controlled to be higher than the glass transition temperature.

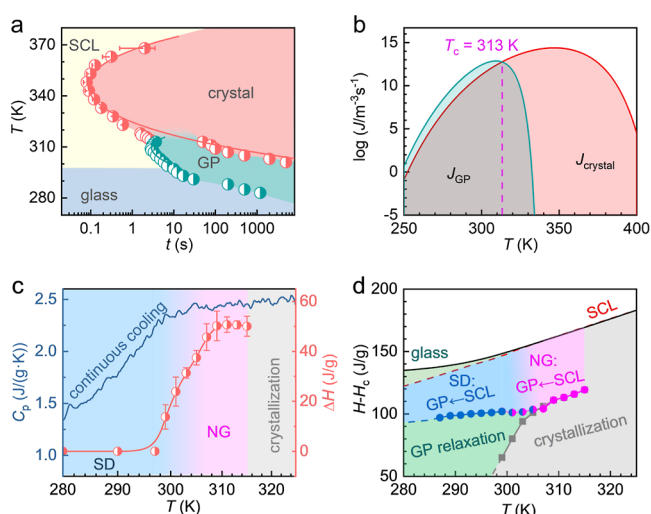


Figure 5. (a) The isothermal transformation diagram of the SCL with a cooling rate of 500 K/s. The red and blue semicircles represent the onset time of the crystallization and the glacial phase formation, respectively. (b) The nucleation rate of the glacial phase (GP) and the crystal changed with temperature. (c) The relationship between the enthalpy change (ΔH) of the liquid–liquid transition and glass transition upon cooling. The red semicircles represent the ΔH changes with temperature. The blue line indicates the variation in heat capacity during the cooling process. (d) The liquid–liquid transition diagram in the enthalpy–temperature space. The vertical axis represents the enthalpy subtracted from the enthalpy of the crystallized sample. The gray squares indicate the onset of the crystallization at different temperatures and also represent the equilibrium state of the GP. The red and blue circles represent the enthalpy values when the SCL is completely transformed to the GP through NG (nucleation and growth) and SD (spinodal decomposition) types, where the sample no longer contains SCL and the heating curve shows a single peak corresponding to the melting of the GP. The red and blue shaded regions denote the transition between the two transformation types.

at T_g .^{23,24} However, the transition to the glacial phase takes about 8 s, which is much shorter than τ_α . This suggests that the formation of the glacial phase should not be related to the long-range cooperative α relaxation.

The nucleation kinetics of the glacial phase and crystallization of D-mannitol was studied. Figure S3 shows the fitting result of the time–temperature transition curves based on the

classical nucleation theory.^{25,26} For the fragile D-mannitol liquid, the temperature dependence of viscosity was corrected using the method proposed by M.D. Ediger et al.²⁷ The detailed information can be found in the Supporting Information. The derived nucleation rate J of the crystallization and glacial phase formation is given in Figure 5b. It can be found that the J_{crystal} and J_{GP} intersected at $T = 313$ K, where the glacial phase began to form. And the higher J_{GP} at lower temperatures compared to J_{crystal} might be related to the structural heterogeneity observed in Figure 2b. Moreover, the interfacial energy of the glacial phase obtained by the fitting was 14.1 mJ/m^2 , much lower than the 31.9 mJ/m^2 for crystallization.

Generally, LLT can be classified into two types, nucleation–growth (NG) and spinodal decomposition (SD), by the evolution of the onset temperature of glass transition with annealing time.^{14,15} The critical temperature for the transition from NG to SD in D-mannitol was between 295 and 300 K.^{14,15} Here, the enthalpy ΔH of the exothermic peak observed in the LLT was calculated, as shown in Figure 5c. Interestingly, the ΔH approached zero precisely in the range of 295 to 300 K, indicating that the observed exothermic peak represents an NG-type LLT. The variation of the ΔH provides a more intuitive basis for distinguishing the LLT types. Additionally, the blue curve in Figure 5c represents the heat capacity C_p of SCL during continuous cooling near the glass transition. It can be observed that the critical temperature for the NG to SD type was approximately equal to the onset of the glass transition. This denotes that the slow atomic diffusivity below the glass transition is probably a key reason for triggering the SD phase transition.

The LLT diagram in the enthalpy–temperature coordinate system is summarized in Figure 5d. At temperatures higher than the T_g , the SCL will transform to the glacial phase through a NG-type phase transition. After the glacial phase reaches equilibrium, it finally crystallizes. Below T_g , the as-cooled glass will relax toward the SCL, and then the SCL transforms to a glacial phase through the SD type. After the transition from SCL to the glacial phase is finished, the glacial phase crystallizes to a lower energy state.

CONCLUSIONS

In this paper, the structure of the D-mannitol glacial phase and the kinetics of the transition between the glacial phase and

SCL are studied systemically by using flash DSC and cold-field TEM. The glacial phase is a fluctuating spinodal-like structure, representing an intermediate state between the disordered glass and crystal. Moreover, the glacial phase melts in a first-order-like transition at 310 K that is approximately 110 K lower than the normal melting temperature. Phase diagrams are constructed in enthalpy space and temperature–time diagram. Our findings provide new insights into the liquid–liquid transition and glass transition of D-mannitol.

■ ASSOCIATED CONTENT

SI Supporting Information

The Supporting Information is available free of charge at <https://pubs.acs.org/doi/10.1021/acs.jpcb.4c06398>.

Heat flow curves of D-mannitol annealed at different annealing temperatures T_a , recovery experiment of the melting process, and fitting process of time–temperature transition (TTT) curves (PDF)

■ AUTHOR INFORMATION

Corresponding Authors

Lijian Song – CAS Key Laboratory of Magnetic Materials and Devices, and Zhejiang Province Key Laboratory of Magnetic Materials and Application Technology, Ningbo Institute of Materials Technology and Engineering, Chinese Academy of Sciences, Ningbo 315201, China; Center of Materials Science and Optoelectronics Engineering, University of Chinese Academy of Sciences, Beijing 100049, China; Email: songlj@nimte.ac.cn

Jun-Qiang Wang – CAS Key Laboratory of Magnetic Materials and Devices, and Zhejiang Province Key Laboratory of Magnetic Materials and Application Technology, Ningbo Institute of Materials Technology and Engineering, Chinese Academy of Sciences, Ningbo 315201, China; Center of Materials Science and Optoelectronics Engineering, University of Chinese Academy of Sciences, Beijing 100049, China; orcid.org/0000-0002-8066-6237; Email: jqwang@nimte.ac.cn

Authors

Jianing Wang – CAS Key Laboratory of Magnetic Materials and Devices, and Zhejiang Province Key Laboratory of Magnetic Materials and Application Technology, Ningbo Institute of Materials Technology and Engineering, Chinese Academy of Sciences, Ningbo 315201, China; Center of Materials Science and Optoelectronics Engineering, University of Chinese Academy of Sciences, Beijing 100049, China

Xiao Chen – CAS Key Laboratory of Magnetic Materials and Devices, and Zhejiang Province Key Laboratory of Magnetic Materials and Application Technology, Ningbo Institute of Materials Technology and Engineering, Chinese Academy of Sciences, Ningbo 315201, China; Center of Materials Science and Optoelectronics Engineering, University of Chinese Academy of Sciences, Beijing 100049, China

Xiao Jin – CAS Key Laboratory of Magnetic Materials and Devices, and Zhejiang Province Key Laboratory of Magnetic Materials and Application Technology, Ningbo Institute of Materials Technology and Engineering, Chinese Academy of Sciences, Ningbo 315201, China; Center of Materials Science and Optoelectronics Engineering, University of Chinese Academy of Sciences, Beijing 100049, China

Meng Gao – CAS Key Laboratory of Magnetic Materials and Devices, and Zhejiang Province Key Laboratory of Magnetic Materials and Application Technology, Ningbo Institute of Materials Technology and Engineering, Chinese Academy of Sciences, Ningbo 315201, China; Center of Materials Science and Optoelectronics Engineering, University of Chinese Academy of Sciences, Beijing 100049, China; orcid.org/0000-0001-7124-7244

Juntao Huo – CAS Key Laboratory of Magnetic Materials and Devices, and Zhejiang Province Key Laboratory of Magnetic Materials and Application Technology, Ningbo Institute of Materials Technology and Engineering, Chinese Academy of Sciences, Ningbo 315201, China; Center of Materials Science and Optoelectronics Engineering, University of Chinese Academy of Sciences, Beijing 100049, China; orcid.org/0000-0002-2107-4979

Complete contact information is available at:

<https://pubs.acs.org/doi/10.1021/acs.jpcb.4c06398>

Notes

The authors declare no competing financial interest.

■ ACKNOWLEDGMENTS

J.Q.W. acknowledges the valuable and constructive discussions about D-mannitol with Professors J.H. Perepezko, M. D. Ediger, and L. Yu at the University of Wisconsin—Madison. We have been engaged in many joyful discussions when I was a postdoc in Perepezko's lab. The financial support from the National Natural Science Foundation of China (grant nos. 52231006, 52001319, 92163108, 52271158, 52222105, and 51827801) is appreciated.

■ REFERENCES

- (1) Debenedetti, P. G.; Stillinger, F. H. Supercooled Liquids and the Glass Transition. *nature* **2001**, 410, 259–267.
- (2) Ediger, M. D.; Harrowell, P. Perspective: Supercooled Liquids and Glasses. *J. Chem. Phys.* **2012**, 137, 080901.
- (3) Poole, P. H.; Sciortino, F.; Essmann, U.; Stanley, H. E. Phase Behaviour of Metastable Water. *Nature* **1992**, 360, 324–328.
- (4) Mishima, O.; Stanley, H. E. The Relationship between Liquid, Supercooled and Glassy Water. *Nature* **1998**, 396, 329–335.
- (5) Cohen, I.; Ha, A.; Zhao, X.; Lee, M.; Fischer, T.; Strouse, M. J.; Kivelson, D. A Low-Temperature Amorphous Phase in a Fragile Glass-Forming Substance. *J. Phys. Chem.* **1996**, 100, 8518–8526.
- (6) Tanaka, H.; Kurita, R.; Mataka, H. Liquid-Liquid Transition in the Molecular Liquid Triphenyl Phosphite. *Phys. Rev. Lett.* **2004**, 92, 025701.
- (7) Zhu, M.; Wang, J.-Q.; Perepezko, J. H.; Yu, L. Possible Existence of Two Amorphous Phases of D-Mannitol Related by a First-Order Transition. *J. Chem. Phys.* **2015**, 142, 244504.
- (8) Tang, W.; Perepezko, J. H. Polyamorphism and Liquid-Liquid Transformations in D-Mannitol. *J. Chem. Phys.* **2018**, 149, 074505.
- (9) Lan, S.; Ren, Y.; Wei, X. Y.; Wang, B.; Gilbert, E. P.; Shibayama, T.; Watanabe, S.; Ohnuma, M.; Wang, X. L. Hidden Amorphous Phase and Reentrant Supercooled Liquid in Pd-Ni-P Metallic Glasses. *Nat. Commun.* **2017**, 8, 14679.
- (10) Shen, J.; Lu, Z.; Wang, J.-Q.; Lan, S.; Zhang, F.; Hirata, A.; Chen, M. W.; Wang, X. L.; Wen, P.; Sun, Y. H.; et al. Metallic Glacial Glass Formation by a First-Order Liquid–Liquid Transition. *J. Phys. Chem. Lett.* **2020**, 11, 6718–6723.
- (11) Shen, J.; Sun, Y. H.; Orava, J.; Bai, H. Y.; Wang, W. H. Liquid-to-Liquid Transition around the Glass-Transition Temperature in a Glass-Forming Metallic Liquid. *Acta Mater.* **2022**, 225, 117588.
- (12) Luan, H.; Zhang, X.; Ding, H.; Zhang, F.; Luan, J. H.; Jiao, Z. B.; Yang, Y. C.; Bu, H.; Wang, R.; Gu, J.; et al. High-Entropy Induced

a Glass-to-Glass Transition in a Metallic Glass. *Nat. Commun.* **2022**, *13*, 2183.

(13) Yang, Q.; Yang, X.-M.; Zhang, T.; Liu, X.-W.; Yu, H.-B. Structure and Entropy Control of Polyamorphous Transition in High-Entropy Metallic Glasses. *Acta Mater.* **2024**, *266*, 119701.

(14) Kobayashi, M.; Tanaka, H. The Reversibility and First-Order Nature of Liquid-Liquid Transition in a Molecular Liquid. *Nat. Commun.* **2016**, *7*, 13438.

(15) Cao, C. R.; Tang, W.; Perepezko, J. H. Liquid-Liquid Transition Kinetics in D-Mannitol. *J. Chem. Phys.* **2022**, *157*, 071101.

(16) An, Q.; Johnson, W. L.; Samwer, K.; Corona, S. L.; Goddard, W. A. First-Order Phase Transition in Liquid Ag to the Heterogeneous G-Phase. *J. Phys. Chem. Lett.* **2020**, *11*, 632–645.

(17) Liu, S. L.; Zhang, H. P.; Sun, B. Y.; Sun, Y. H.; Bai, H. Y.; Wang, W. H. Glassy or Amorphous? A Demonstration Using G-Phase Copper Containing a Fivefold Twinning Structure. *J. Phys. Chem. Lett.* **2022**, *13*, 754–762.

(18) Kawasaki, T.; Tanaka, H. Formation of a Crystal Nucleus from Liquid. *Proc. Natl. Acad. Sci. U.S.A.* **2010**, *107*, 14036–14041.

(19) Gee, R. H.; Lacevic, N.; Fried, L. E. Atomistic Simulations of Spinodal Phase Separation Preceding Polymer Crystallization. *Nat. Mater.* **2006**, *5*, 39–43.

(20) Vega, D. A.; Gómez, L. R. Spinodal-Assisted Nucleation During Symmetry-Breaking Phase Transitions. *Phys. Rev. E* **2009**, *79*, 051607.

(21) Xu, Y.; Wang, Y.; Xu, T.; Zhang, J.; Liu, C.; Shen, C. Crystallization Kinetics and Morphology of Partially Melted Poly-(Lactic Acid). *Polym. Test.* **2014**, *37*, 179–185.

(22) Song, G.; Hogan, C. J. Crystal Grain Size Effects and Crystallinity Dynamics During Supersonic Particle Impacts. *Int. J. Plast.* **2023**, *170*, 103758.

(23) Angell, C. A. Relaxation in Liquids, Polymers and Plastic Crystals - Strong/Fragile Patterns and Problems. *J. Non-Cryst. Solids* **1991**, *131–133*, 13–31.

(24) Angell, C. A.; Ngai, K. L.; McKenna, G. B.; McMillan, P. F.; Martin, S. W. Relaxation in Glassforming Liquids and Amorphous Solids. *J. Appl. Phys.* **2000**, *88*, 3113–3157.

(25) Perepezko, J. H.; Hildal, K. Analysis of Solidification Microstructures During Wedge-Casting. *Philos. Mag.* **2006**, *86*, 3681–3701.

(26) Perepezko, J. H.; Santhaweesuk, C.; Wang, J. Q.; Imhoff, S. D. Kinetic Competition During Glass Formation. *J. Alloy. Compd.* **2014**, *615*, S192–S197.

(27) Ediger, M. D.; Harrowell, P.; Yu, L. Crystal Growth Kinetics Exhibit a Fragility-Dependent Decoupling from Viscosity. *J. Chem. Phys.* **2008**, *128*, 034709.